Mars Atmosphere and Volatile EvolutioN (MAVEN) Mission

# Impact ionization of neutrals by foreshock electrons at Mars

Christian Mazelle[1], Karim Meziane[1,2], Dave L. Mitchell[3], Philippe Garnier[1], Jared R. Espley[4], Abdelhaq Hamza[2], Jasper S. Halekas[5], and Bruce M. Jakosky[6]

[1] IRAP, CNRS – University of Toulouse, UPS, CNES, France; [2] Physics Department, University of New Brunswick, Fredericton, Canada; [3] Space Sciences Laboratory, University of California, Berkeley, USA; [4] NASA Goddard Space Flight Center, Greenbelt, MD, USA; [5] Department of Physics and Astronomy, University of Iowa, Iowa City, USA; [6] LASP, University of Colorado, Boulder, USA

*ESLAB-52nd Symposium: Comparative Aeronomy and Plasma Environments of Terrestrial Planets, Symposium, ESA/ESTEC, Noordwijk, The Netherlands, May 14-18, 2018*

# Foreshock Geometry

**3 major geometrical parameters:**

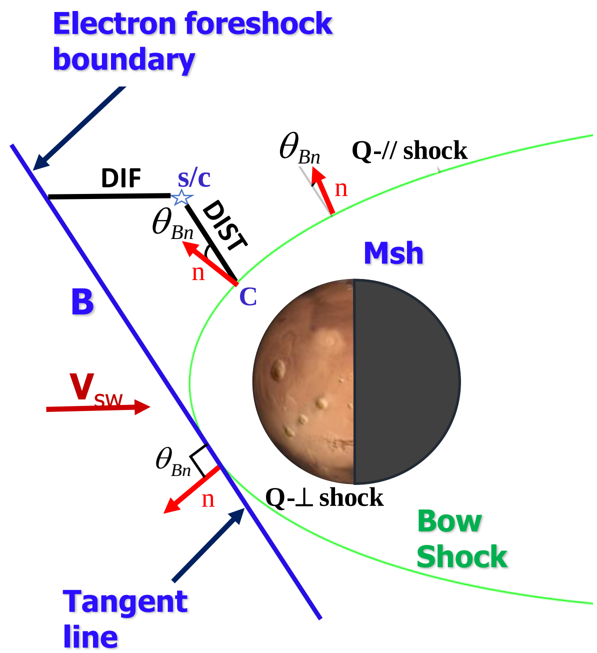


1. $\theta_{Bn}$ : Angle between the interplanetary magnetic field line and the shock normal at the connection point (model).

2. **DIST** : distance between the s/c and the shock connection point along a straight line parallel to the IMF average.

3. **DIF** : distance of the s/c from the **tangent** field line along the X_MSO axis (Mars–Sun line)
**Depth inside the foreshock (negative if no connection)**

# Foreshock Geometry

**3 major geometrical parameters:**

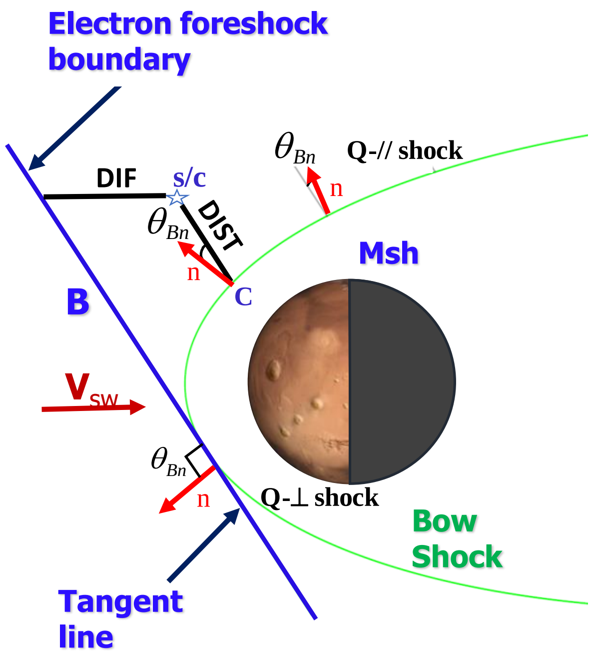


1. $\theta_{Bn}$ : Angle between the interplanetary magnetic field line and the shock normal at the connection point (model).

2. **DIST** : distance between the s/c and the shock connection point along a straight line parallel to the IMF average.

3. **DIF** : distance of the s/c from the **tangent** field line along the X_MSO axis (Mars–Sun line)

**Depth inside the foreshock (negative if no connection)**

Use of a bow shock model [Vignes *et al.*, 2000]
Conic section (axisymetric) from a fit of bow shock crossing locations by Mars Global Surveyor.

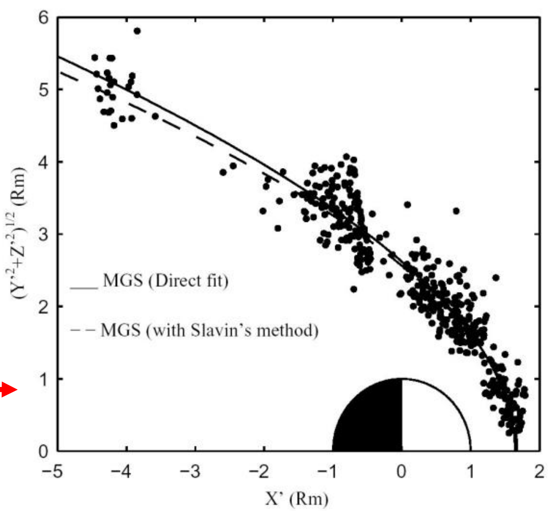

# First Martian electron foreshock study at Mars by MAVEN

Meziane et al., *JGR*, 2017

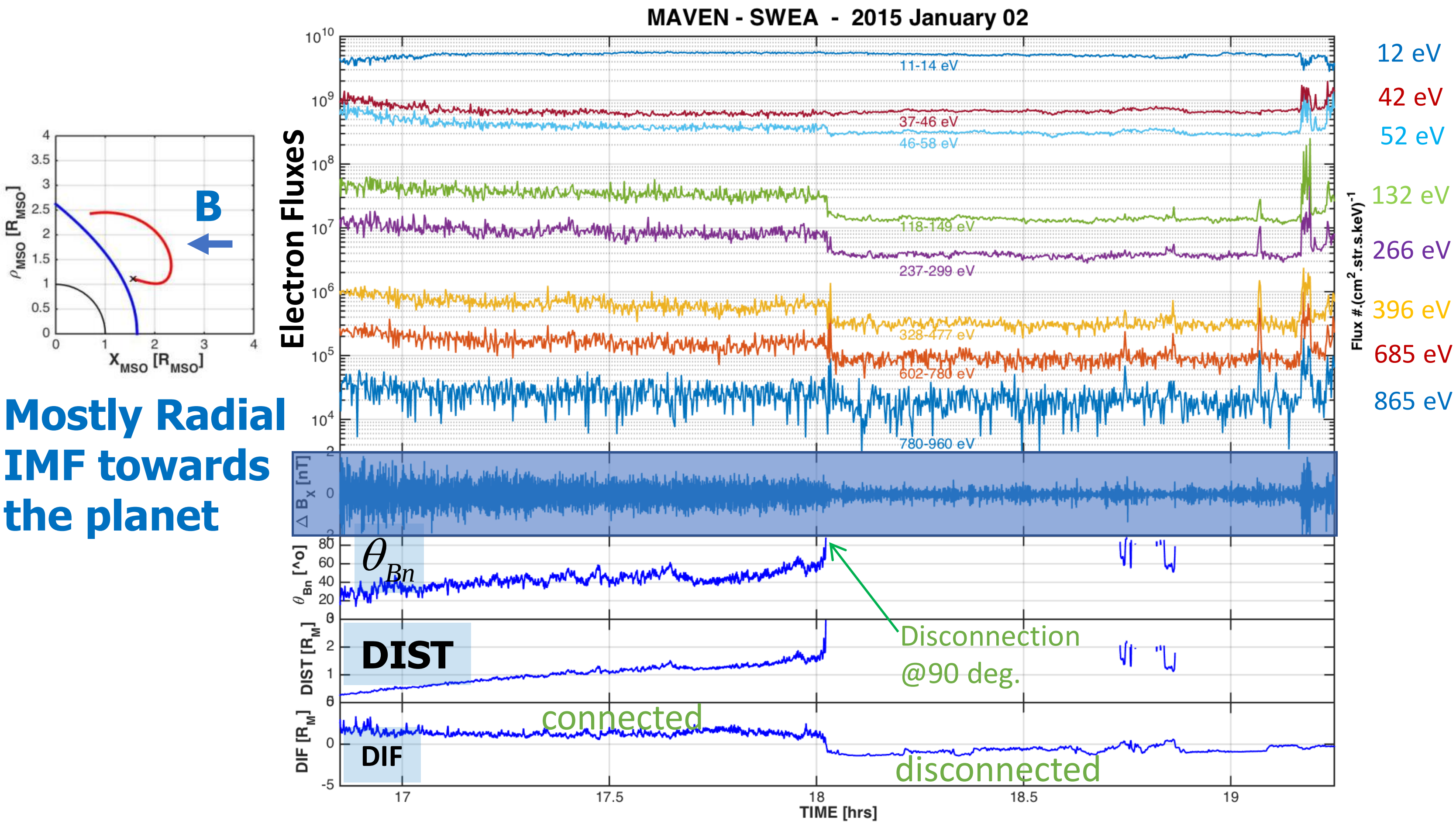


**Mostly Radial IMF towards the planet**

# Observations vs connection model

Meziane et al., *JGR*, 2017

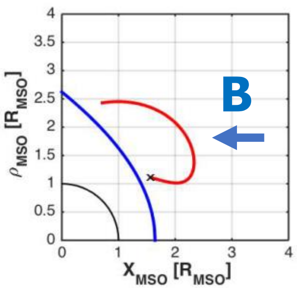


**Mostly Radial IMF towards the planet**

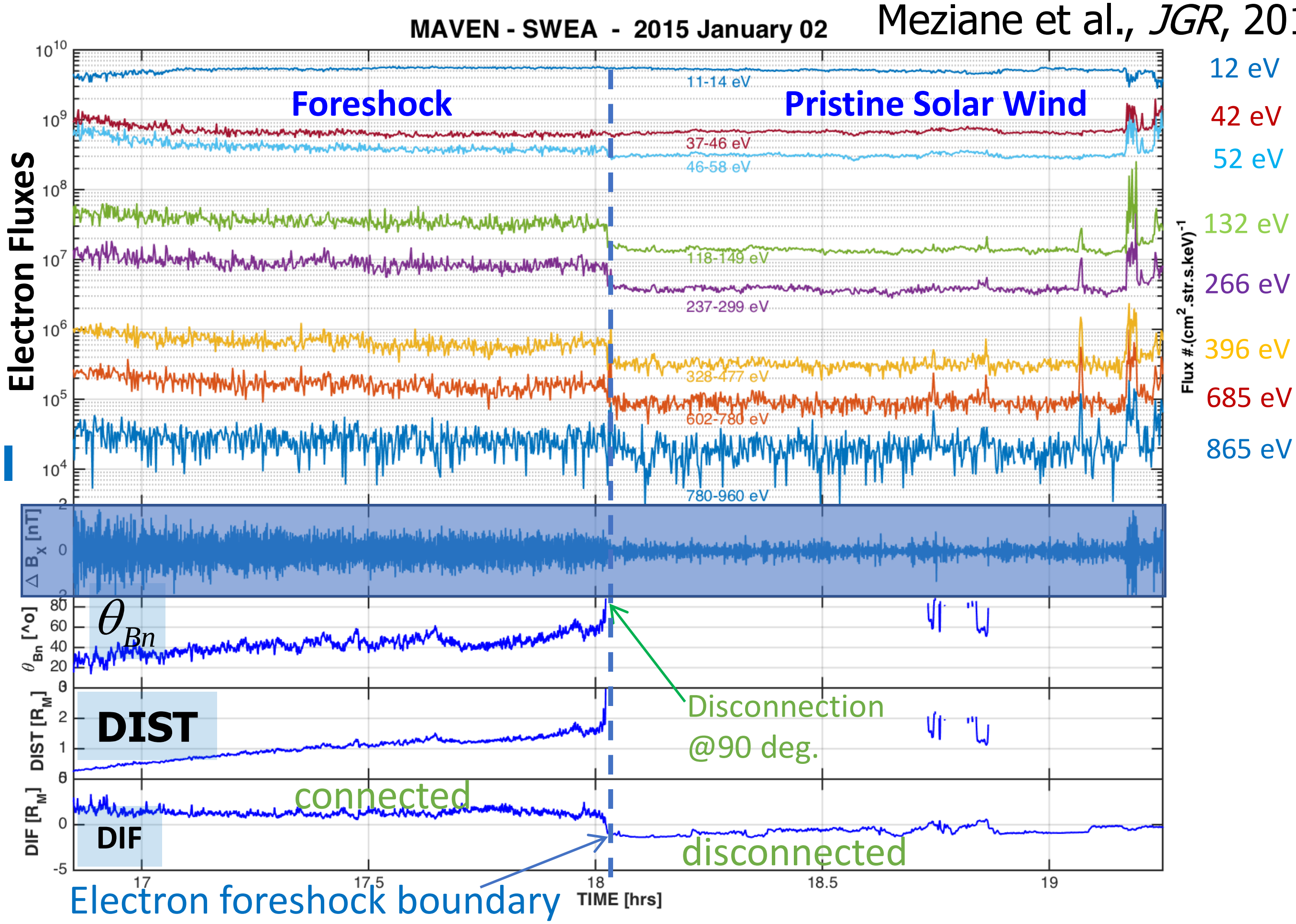

# Production mechanism

## Adiabatic shock reflection: computation of reflected fluxes

Solar wind electrons reflect off the shock in an adiabatic manner (conservation of magnetic moment). The pre (post) shock-encounter particle energy $E_i$ ($E$) and pitch angle $\mu_i = \cos\alpha_i$ ($\mu = \cos\alpha$) in the plasma frame of reference are given by:

$$\frac{E_i}{E} = 1 + 4\times\frac{E_S}{E} - 4\times\mu\times\sqrt{\frac{E_S}{E}} \qquad \mu_i = \frac{\mu - \sqrt{\frac{E_S}{E}}}{\sqrt{\frac{E_i}{E}}}$$

$E_s$ = Energy corresponding to the shock speed $V_s$ :

$$\mathbf{V}_S = \mathbf{V}_{SW} - \mathbf{V}_{dHT} \qquad V_S = V_{SW} \times \frac{\cos\theta_{Vn}}{\cos\theta_{Bn}}$$

Conservation of phase-space density along the orbit (**Liouville's theorem**):

$$f_r(E,\mu) = f_{SW}(E_i(E,\mu),\mu_i(E,\mu))$$

$f_{SW}$ : seed population obtained by fitting with a kappa distribution of a pristine solar wind distribution.

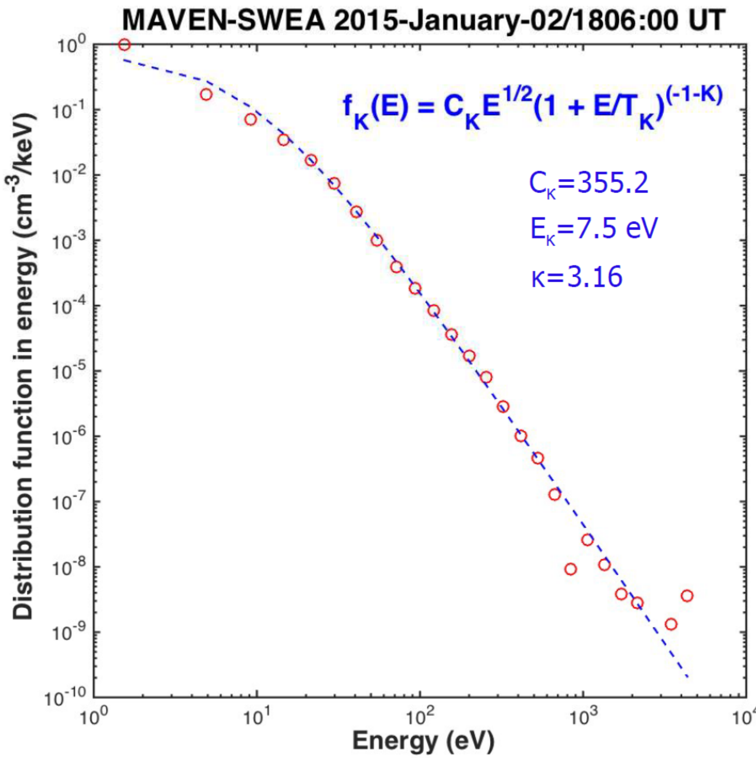

# Production mechanism

## Adiabatic shock reflection: computation of reflected fluxes

Solar wind electrons reflect off the shock in an adiabatic manner (conservation of magnetic moment). The pre (post) shock-encounter particle energy $E_i$ ($E$) and pitch angle $\mu_i = \cos\alpha_i$ ($\mu = \cos\alpha$) in the plasma frame of reference are given by:

$$\frac{E_i}{E} = 1 + 4 \times \frac{E_S}{E} - 4 \times \mu \times \sqrt{\frac{E_S}{E}} \qquad \mu_i = \frac{\mu - \sqrt{\frac{E_S}{E}}}{\sqrt{\frac{E_i}{E}}}$$

$E_s$ = Energy corresponding to the shock speed $V_s$ :

$$\mathbf{V}_S = \mathbf{V}_{SW} - \mathbf{V}_{dHT} \qquad V_S = V_{SW} \times \cos\theta_{Vn} / \cos\theta_{Bn}$$

Conservation of phase-space density along the orbit (**Liouville's theorem**):

$$f_r(E,\mu) = f_{SW}(E_i(E,\mu), \mu_i(E,\mu))$$

$f_{SW}$ : seed population obtained by fitting with a kappa distribution of a pristine solar wind distribution.

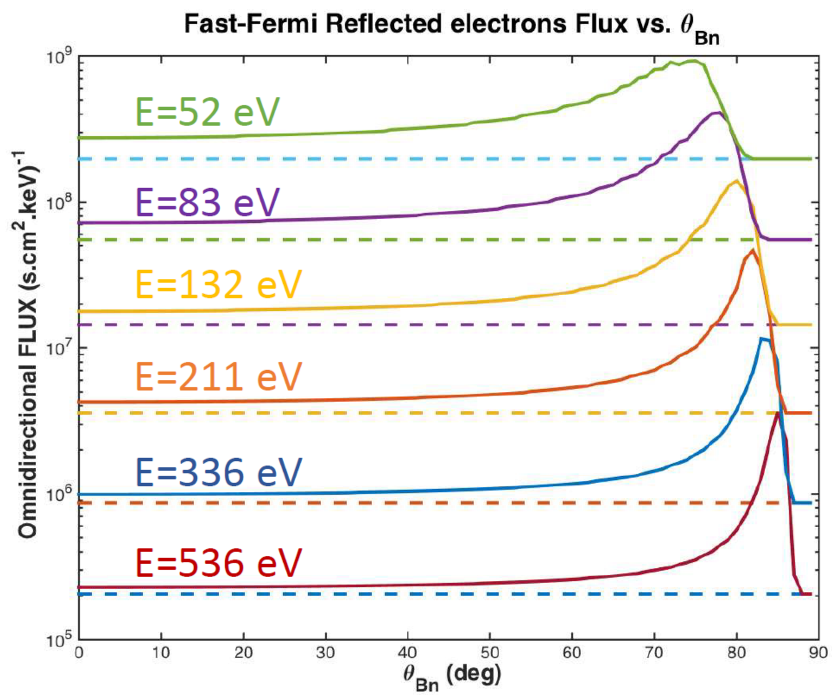


**Fluxes increase with $\theta_{Bn}$**

# Puzzling observations

**(1)**

**Flux fall-off above ~30 eV when $\theta_{Bn}$ increases !**

Meziane et al., *JGR*, 2017

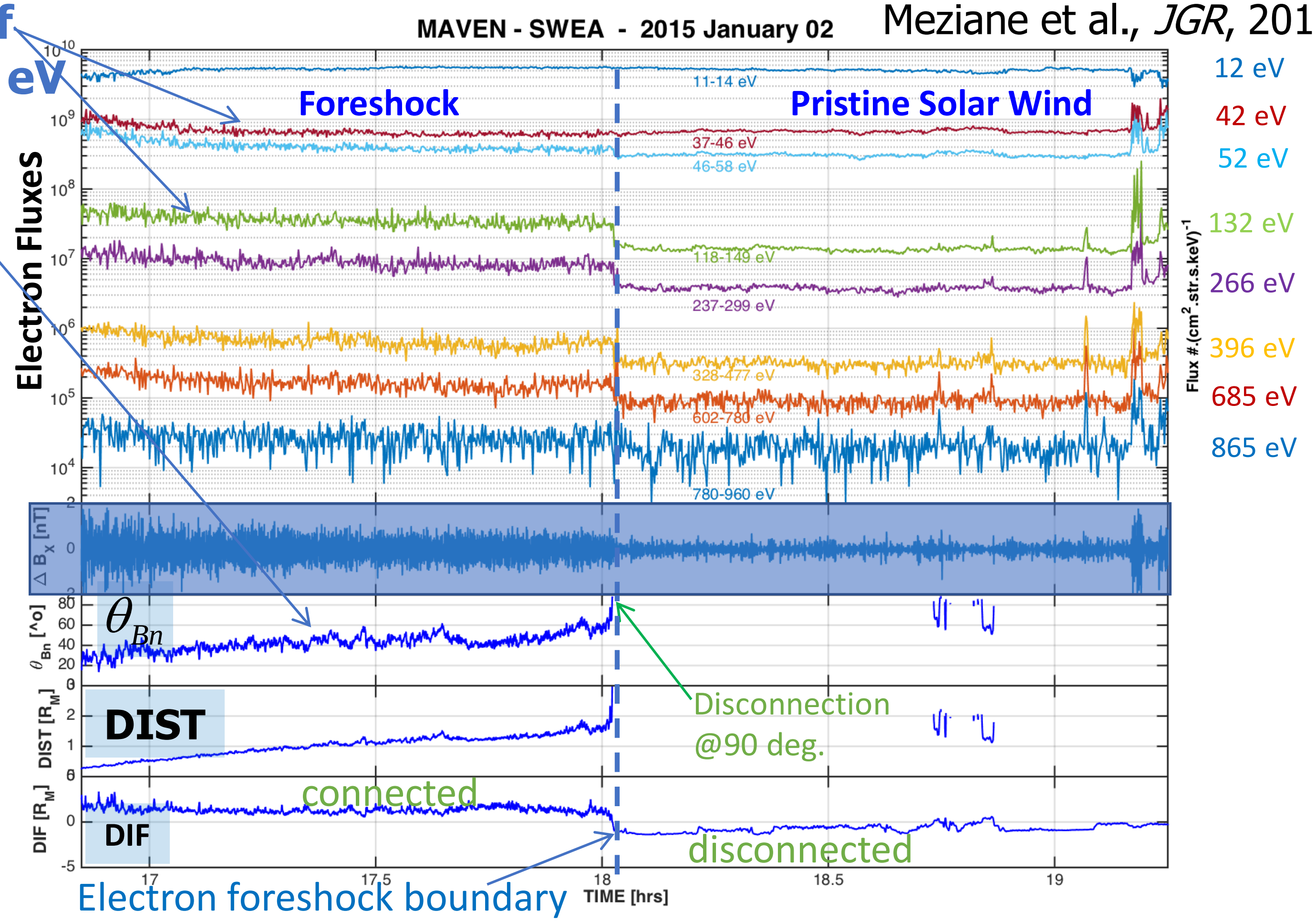


Apparent discrepancy with the theory for the variation versus $\theta_{Bn}$ !... Why?

# Puzzling observations

**(1)**

**Flux fall-off above ~30 eV when $\theta_{Bn}$ increases ! but also DIST**

Meziane et al., *JGR*, 2017

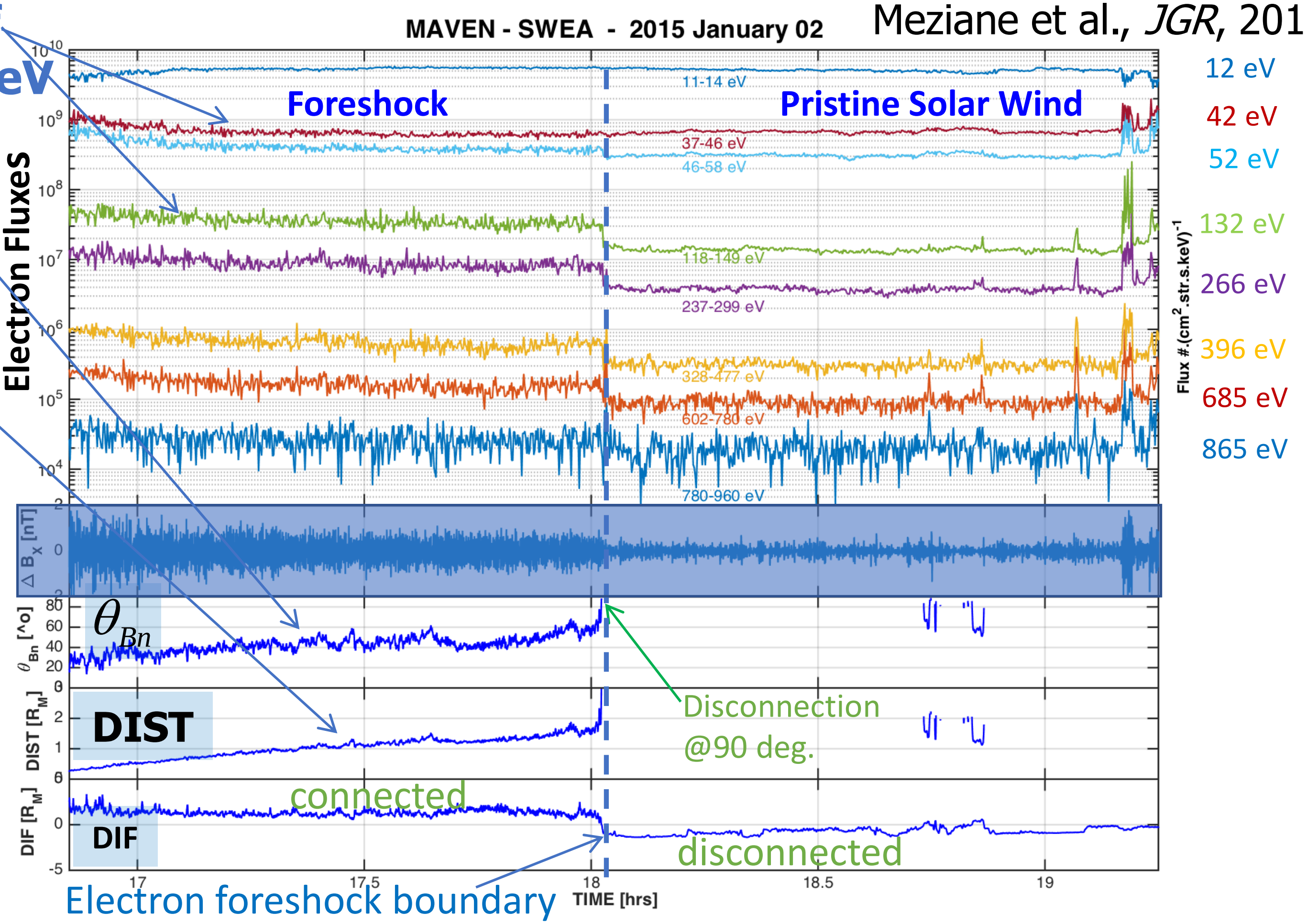


Apparent discrepancy with the theory for the variation versus $\theta_{Bn}$ !... Why?

The distance along the magnetic field is more relevant for the flux decay.

# Puzzling observations

**(1)**
**Flux fall-off above ~30 eV when $\theta_{Bn}$ increases ! but also DIST**

Meziane et al., *JGR*, 2017

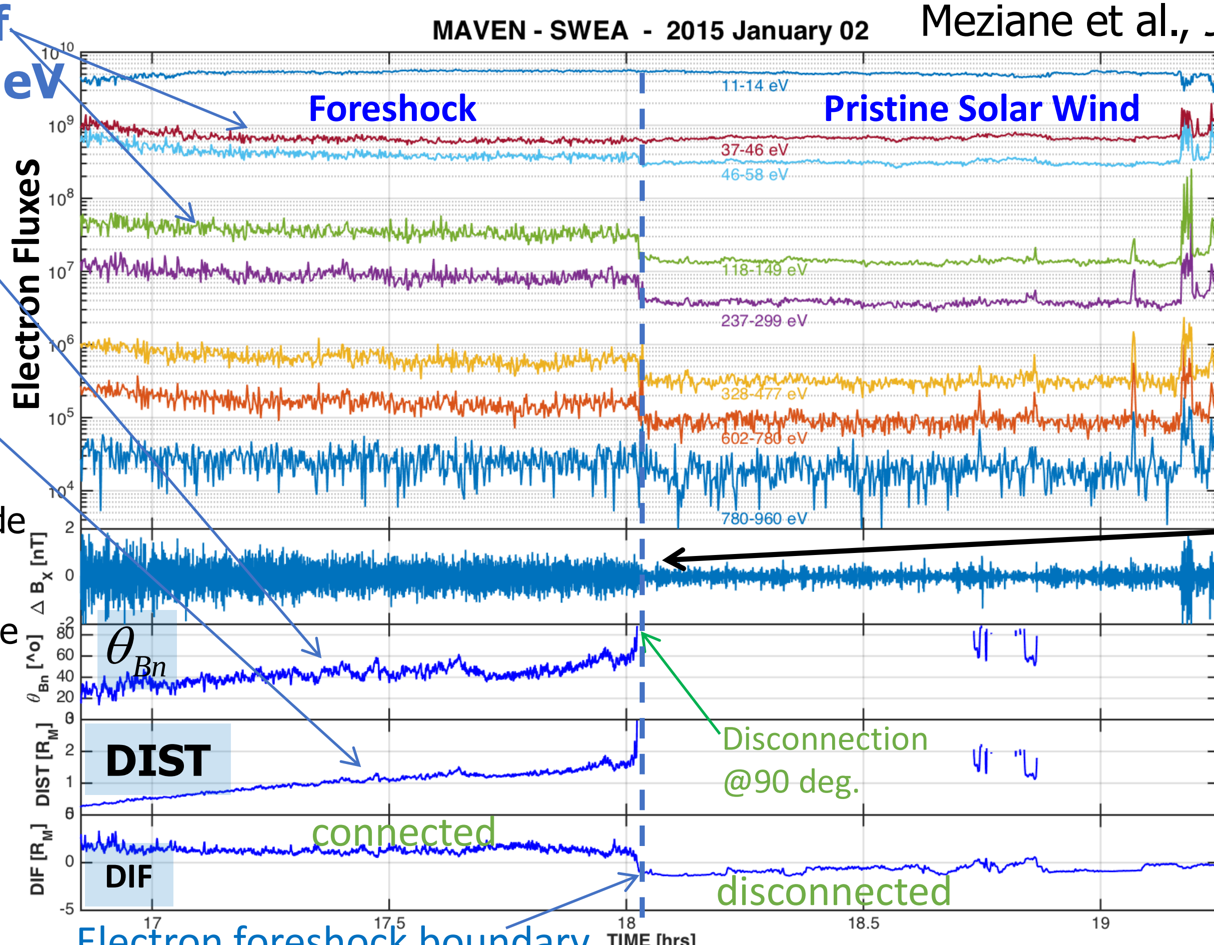


ULF Wave amplitude

$$\Delta \mathbf{B} = \mathbf{B} - \mathbf{B}_0$$

$\mathbf{B}_0$ sliding average

**(2)**
Drop of the amplitude of pickup ions (protons) ULF waves in the pristine SW compared to the foreshock

Systematically observed **when crossing** the FSh boundary

Apparent discrepancy with the theory for the variation versus $\theta_{Bn}$ !… Why?

The distance along the magnetic field is more relevant for the flux decay.

Influence of the foreshock electrons on pickup proton induced waves?

# Magnetic field fluctuations – Flux – Distance

Electrons

ULF Wave amplitude

$$\Delta \mathbf{B} = \mathbf{B} - \mathbf{B}_0$$

$\mathbf{B}_0$ sliding average

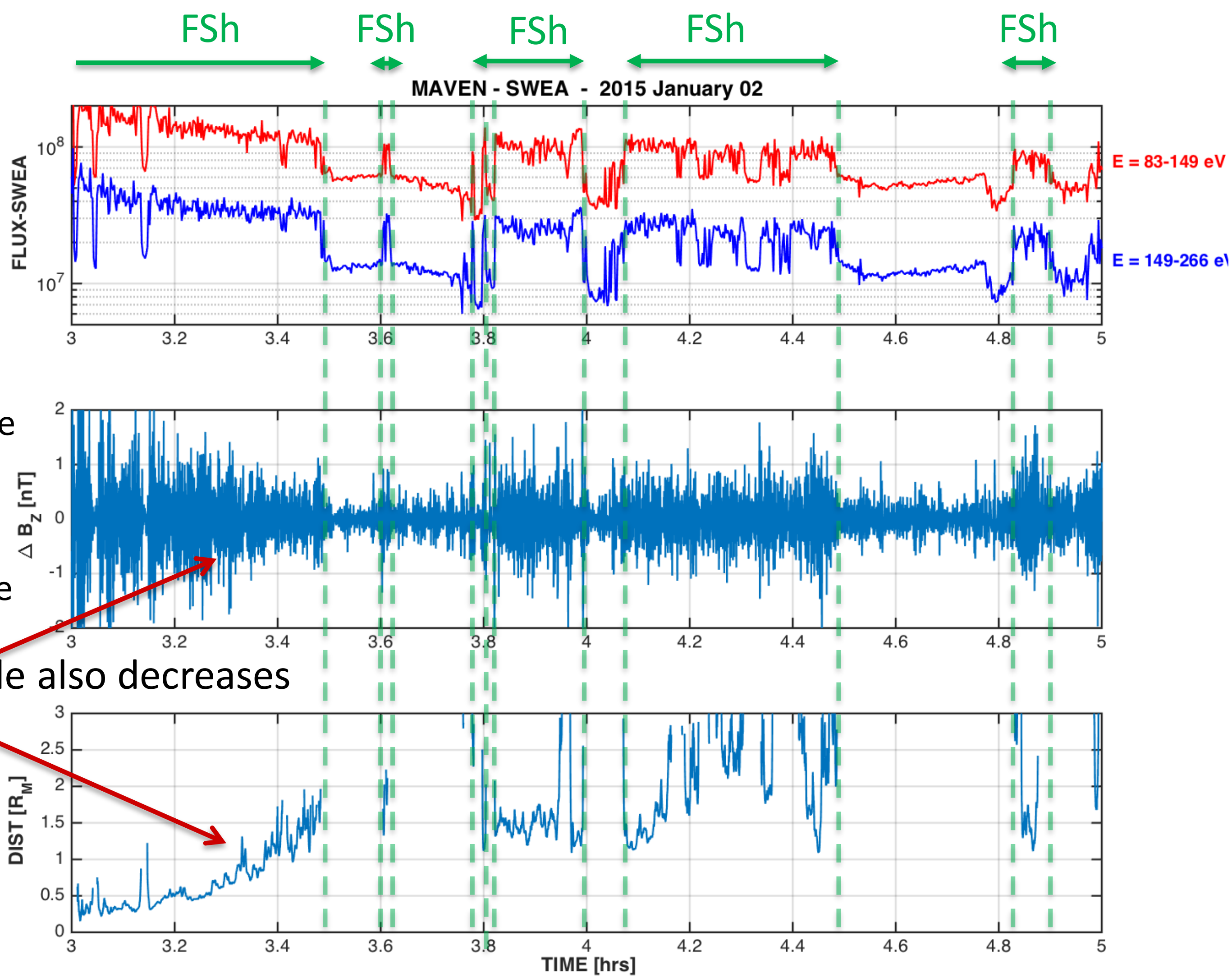


Wave amplitude also decreases with distance along B

Nearly one-to-one correspondance between electron foreshock boundary crossings and amplifications of the planetary pickup protons generated ULF waves.

# other events

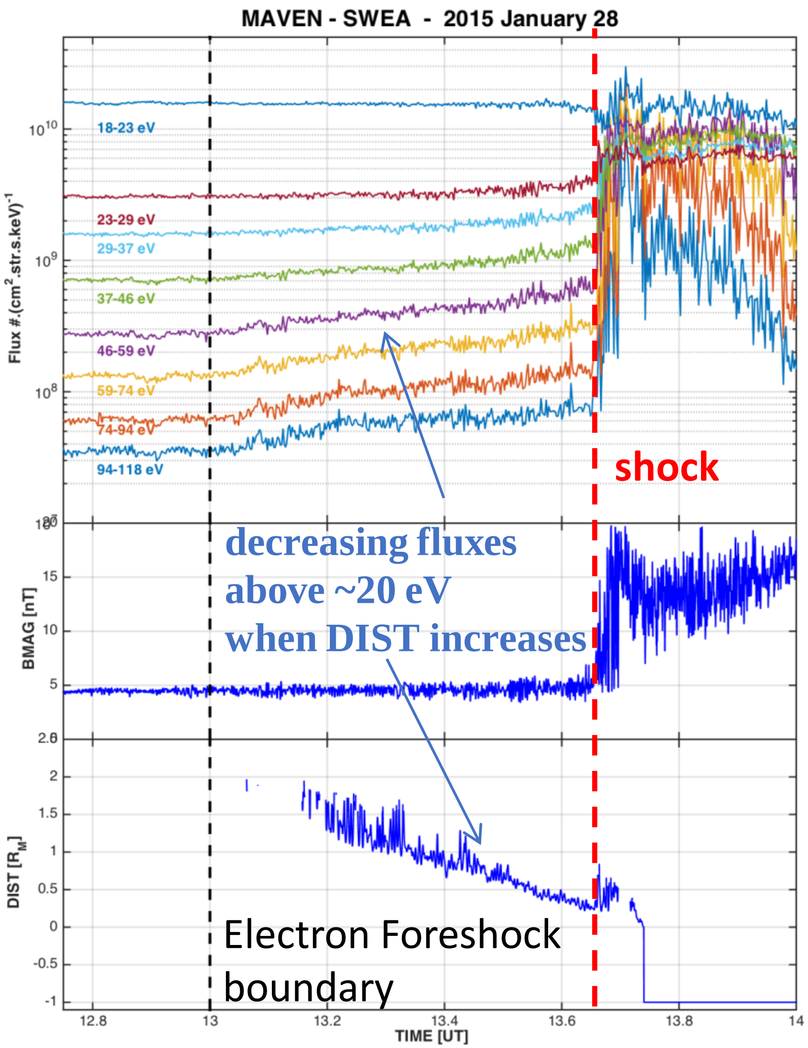


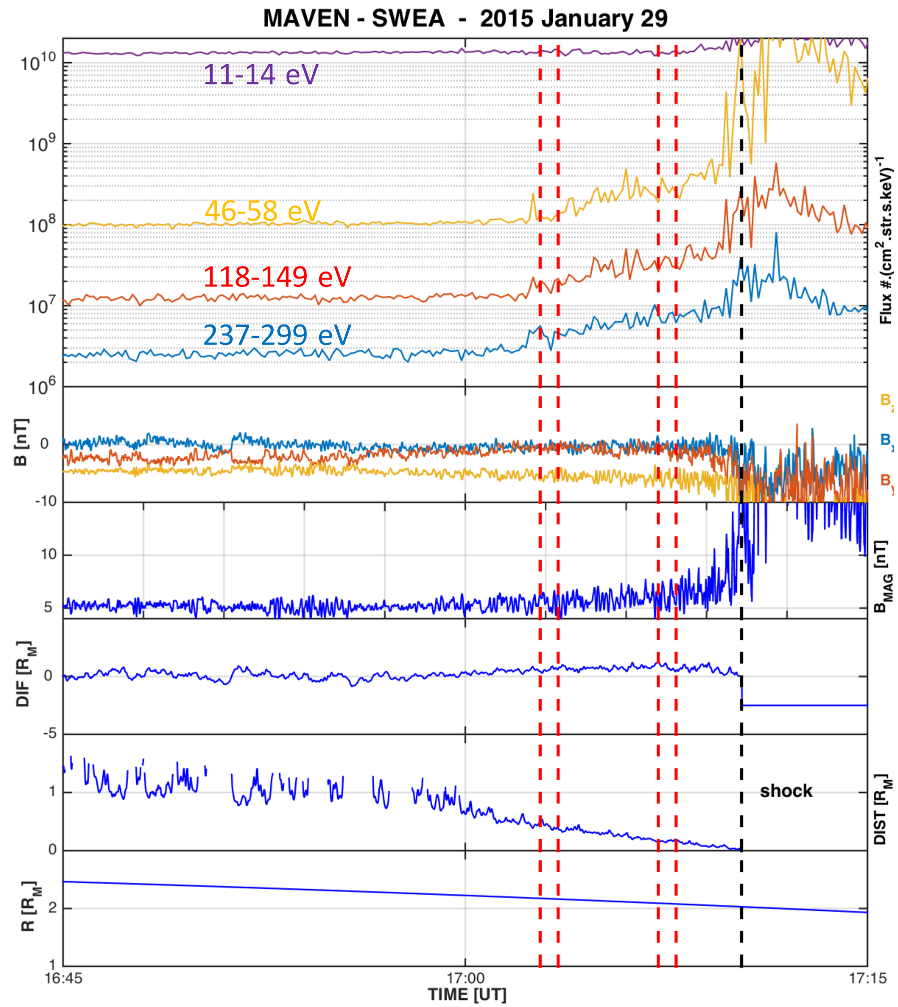


All cases identified up to now and fully analyzed are **always** showing the same feature.

**Too small scale at Mars** to expect an effect of electron microinstabilities (wave generation).

# Martian exosphere

## IUVS Observations of Atomic Components

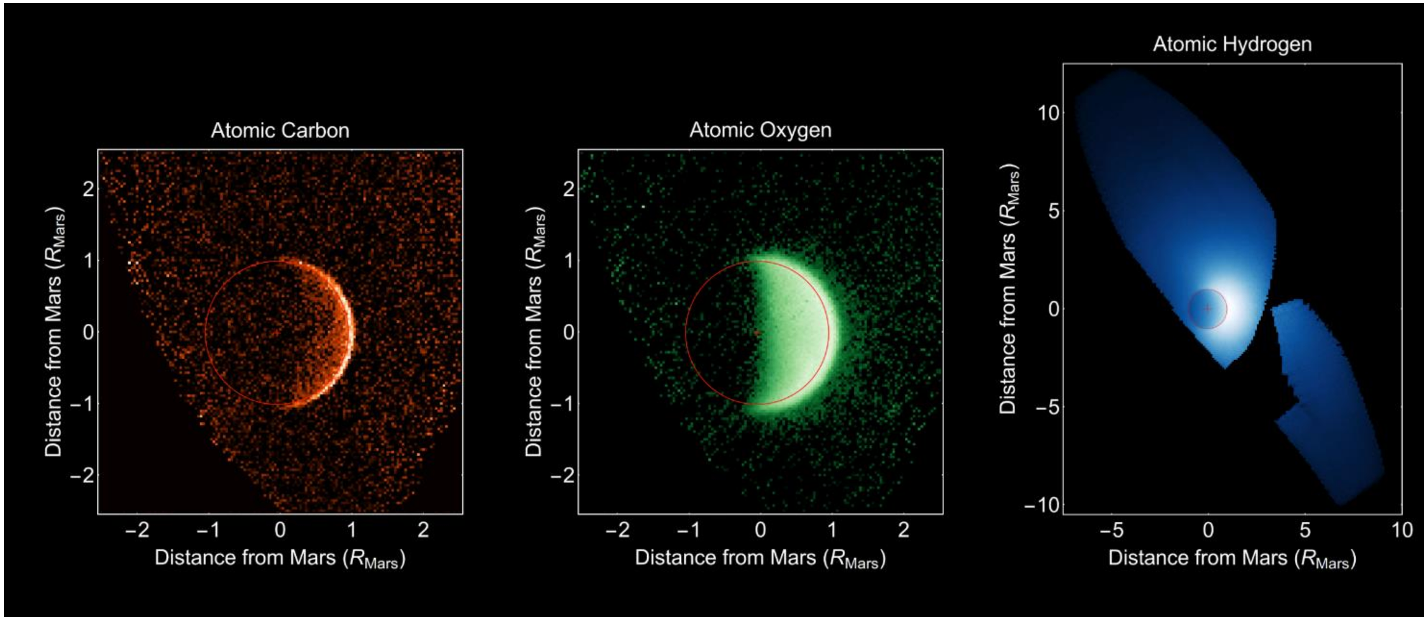


[Chaffin et al. 2015]

Mars has an extended exosphere **expanding far upstream the bow shock** (in particular for H): this is a **source of pickup ions which generate ULF waves** observed at frequencies nearly matching the local ion cyclotron frequencies as for comets [Wu & Davidson, 1972; Gary & Madland, 1988; Brinca, 1991].
Such 'proton cyclotron waves' have been reported at Mars [Russell *et al*., 1990; Brain *et al*., 2002; Bertucci, 2003; Mazelle *et al*., 2004; Wei and Russell, 2006; Wei *et al*., 2011; 2014; Connerney *et al*., 2015; Romanelli *et al*., 2012; 2016; 2018; Bertucci *et al*., 2013; Ruhunusiri *et al*., 2015] from Phobos-2, Mars Global Surveyor and MAVEN observations.

# Pickup proton waves

## An example of PCWs from MAVEN MAG data

Romanelli, et al., JGR, 2017

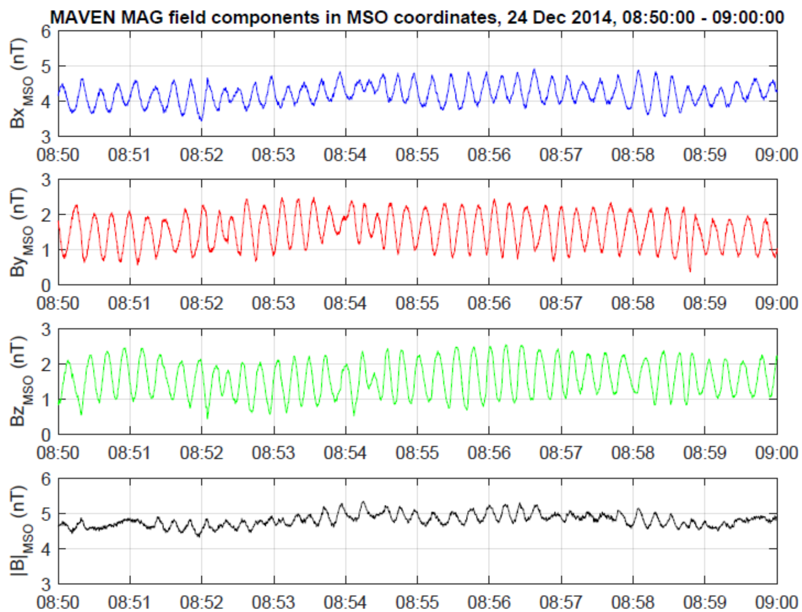


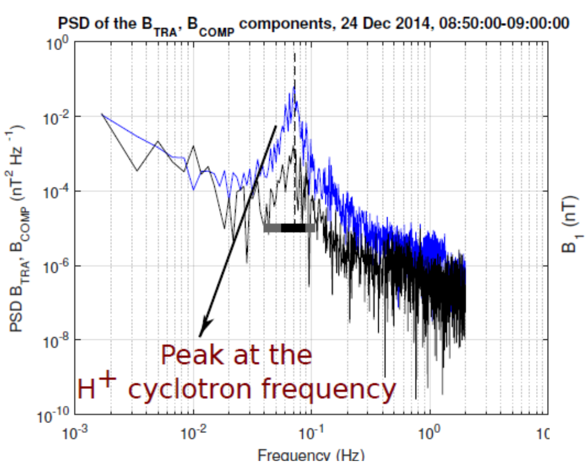


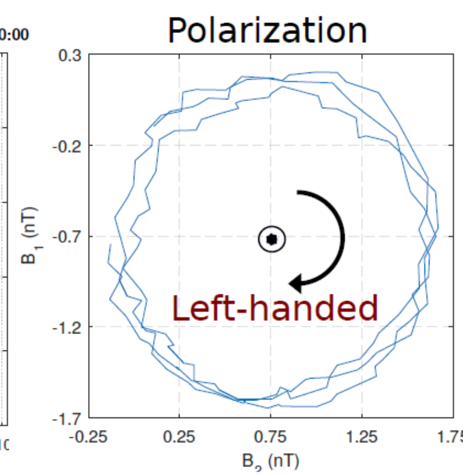

# Wave amplitude amplification in the foreshock

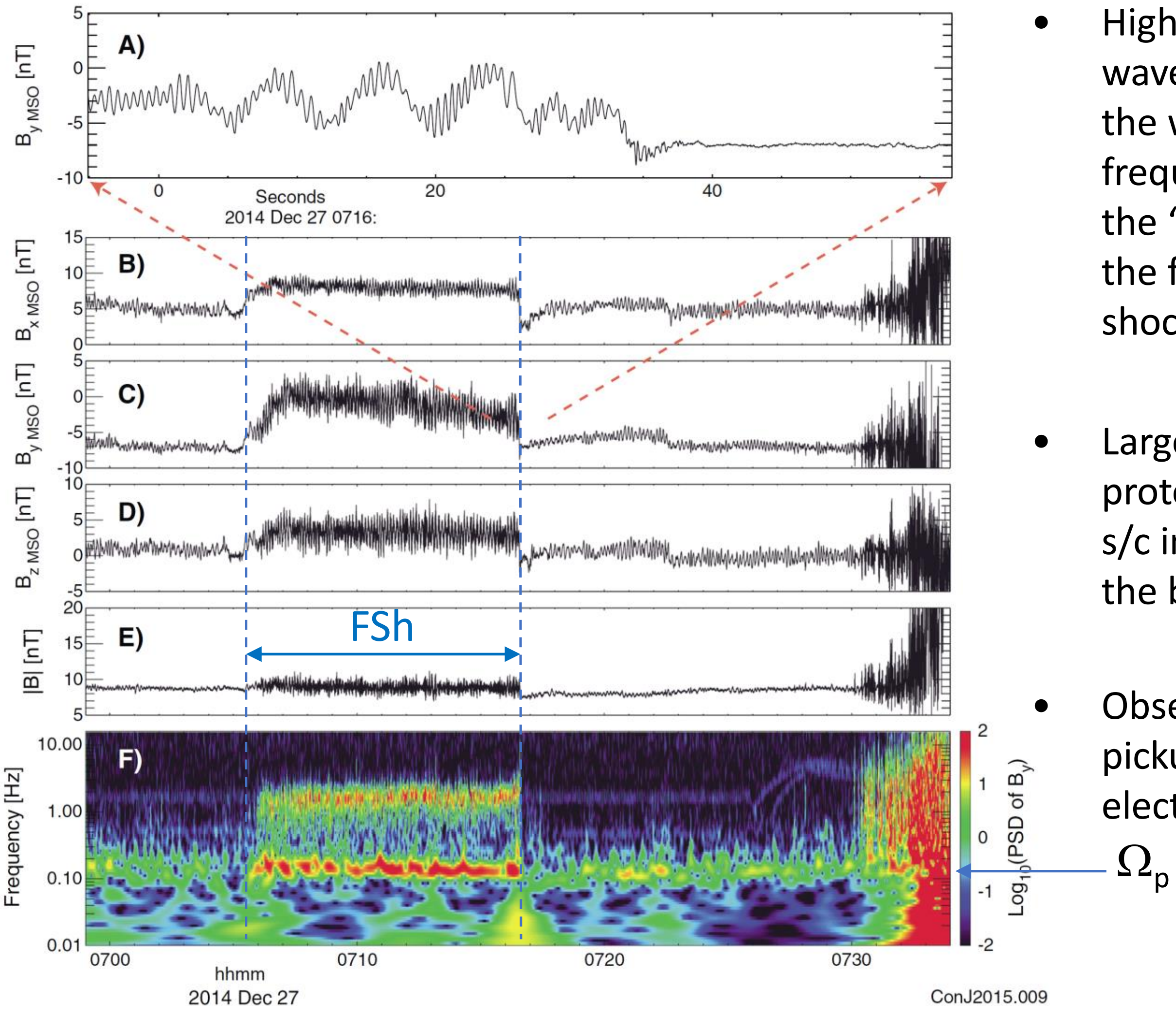


(After Connerney et al., GRL, 2015)

- Higher frequency waves (so called '1 Hz waves' at Earth) seen superimposed on the waves at the proton cyclotron frequency (pickup ions waves). At Earth the '1 Hz' waves are seen only inside the foreshock (most likely source at the shock).
- Larger ULF waves amplitude at the proton cyclotron frequency when the s/c intercepts a field-line connected to the bow shock (electron foreshock).
- Observation consistent with a higher pickup ion production rate inside the electron foreshock.

# Electron Impact Ionization

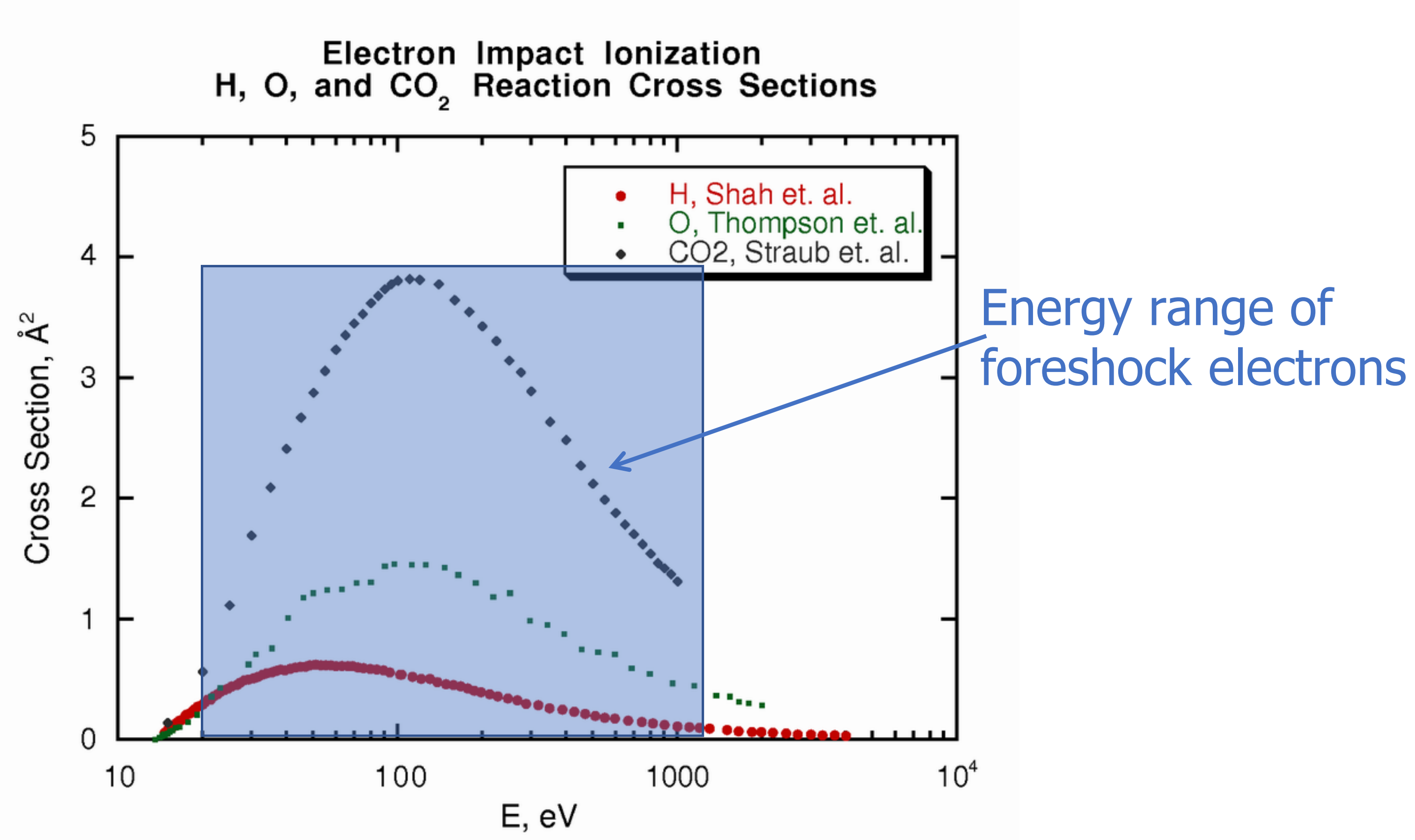


Higher wave amplitude is observed when more energetic electrons are present, so also higher pickup ion density (source of the waves). So this could be due to higher electron impact ionization rate (on H and O non thermal corona).

This needs to be quantified.

# Foreshock Electron Impact Ionization (EII) (1)

- Let us assume that the flux decay with the distance is due to the impact with **exospheric atomic hydrogen** (as a first step).
- Consider a **monoenergetic electron beam** emanating from the shock and moving along the magnetic field.
- At a distance *x*, the flux is $\Gamma_E(x)$, where ***x* is the distance along the ambient magnetic field**.
- The variation of the flux is governed by the following equation:

$$\frac{d\Gamma_E(x)}{\Gamma_E(x)} = -n_H(x)\sigma(E)dx \qquad [1]$$

where $n_H(x)$ is the hydrogen density profile and $\sigma(E)$ is the EII cross-section

Integrating between $x = x_1$ and $x = x_2$

$$Ln\left(\frac{\Gamma_E(x_2)}{\Gamma_E(x_1)}\right) = -\sigma(E)\int_{x_1}^{x_2} n_H(x)dx = -\sigma(E)I(x_1, x_2) \qquad [2]$$

# Foreshock Electron Impact Ionization (EII) (2)

- Let us first assume a simple power law profile for the **exospheric atomic hydrogen density** such as $n_H(x) = cx^{-\alpha}$ , then it gives

$$Ln\left(\frac{\Gamma_E(x_2)}{\Gamma_E(x_1)}\right) = -\frac{c\sigma(E)}{1-\alpha}\left[x_2^{1-\alpha} - x_1^{1-\alpha}\right] \qquad [3]$$

- This can be tested for different energy ranges:

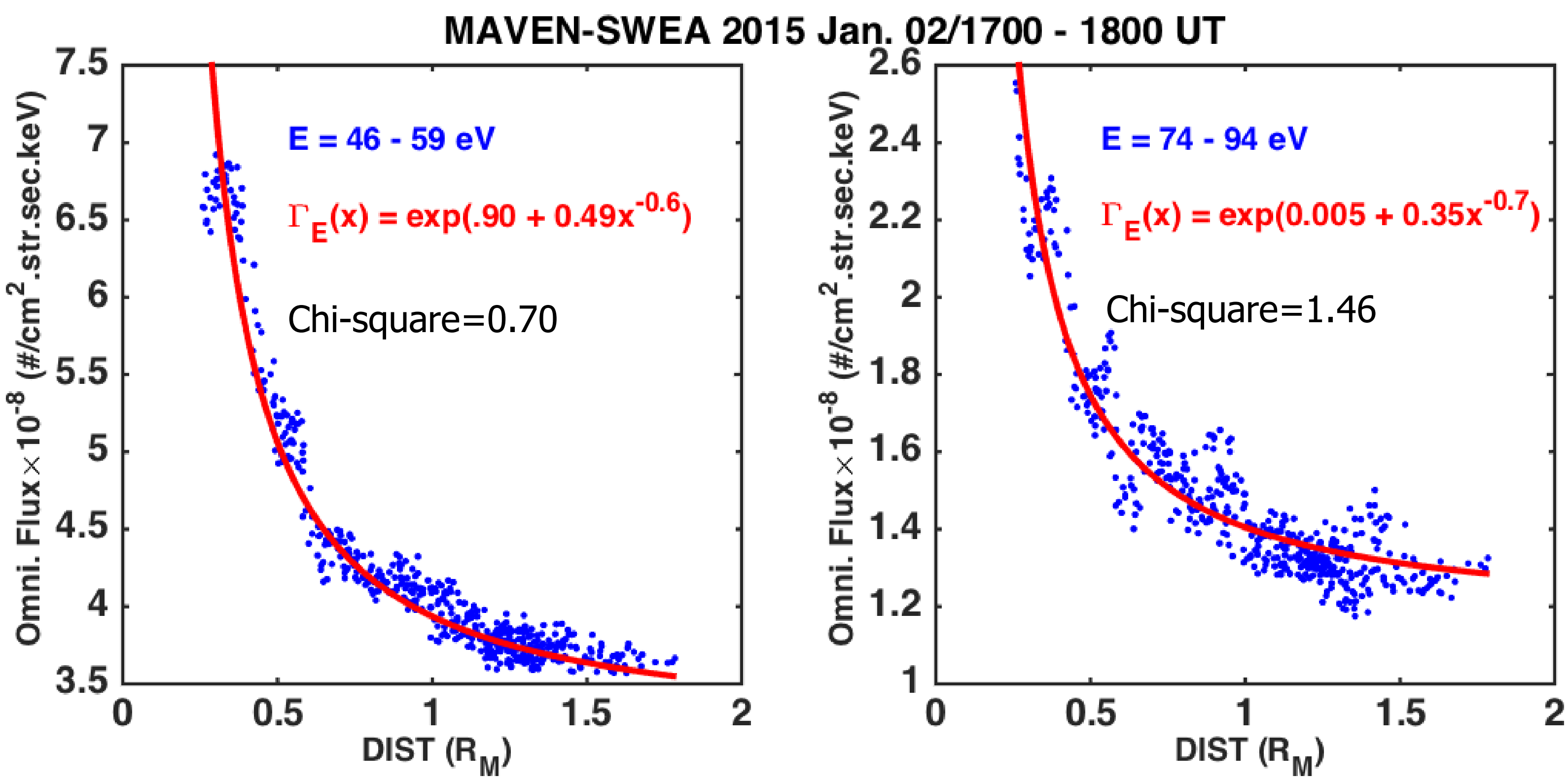


Good agreement: foreshock electrons fluxes attenuation due to EII with neutral H

# Foreshock Electron Impact Ionization (EII) (3)

- Taking the same index as the one derived by Feldman et al. [2011] from Rosetta ALICE measurements: $n_H(r) \propto r^{-2.1}$ where $r$ is the radial distance gives $\Gamma_E(x) \propto \exp(\, a + b\ \ x^{-1.1})$
- It should be a valid approximation only for large distances and B exactly radial so that $r \sim \mathrm{x}$ from the vectorial composition **r** = **ρ** + **x** , where **ρ** is the vector position of the connection point at the shock from the planet center.

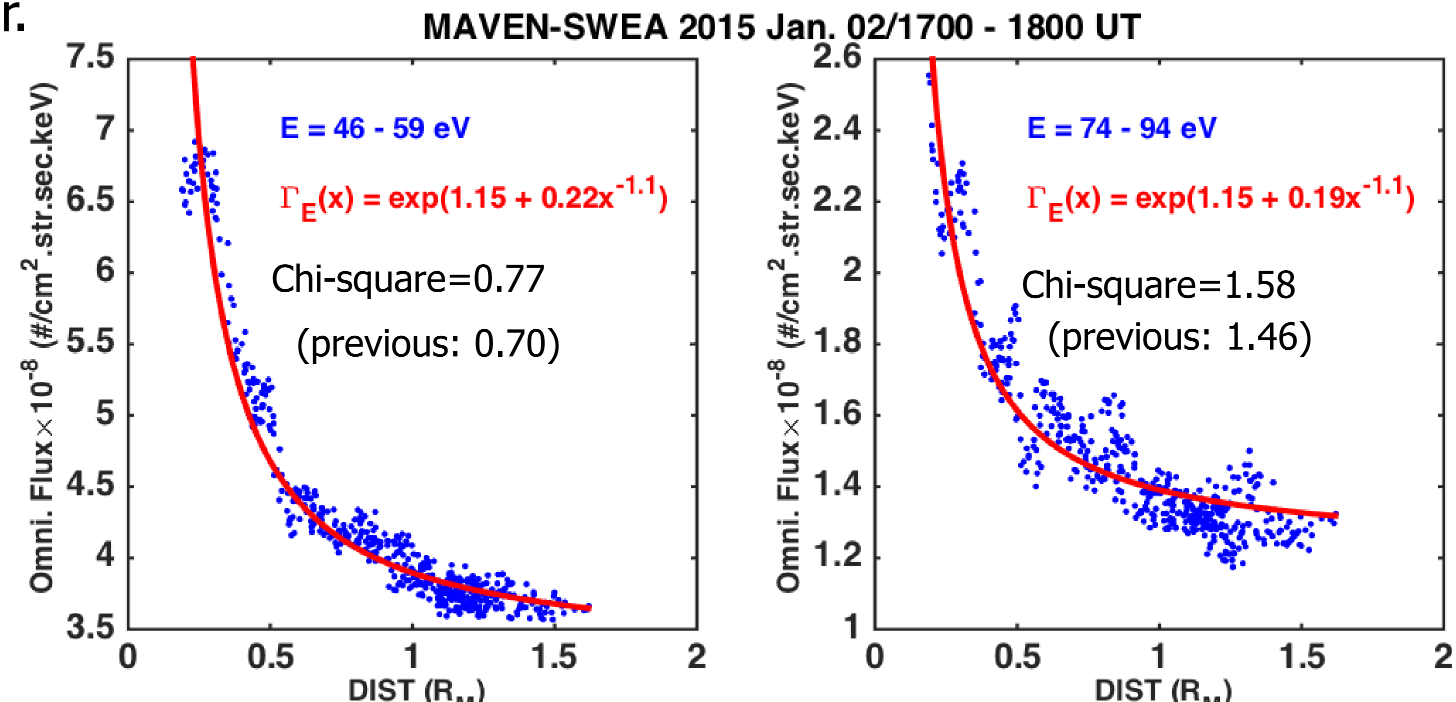


Little less good agreement but still consistent using the 1-D hydrogen radial profile

# Foreshock Electron Impact Ionization (EII) (4)

Pursuing our analysis further and in order to precise the comparison with the model, both the distance and the **exospheric hydrogen density profile** are eliminated from the comparison.

Considering two arbitrary energy channels $E_1$ and $E_2$, let's build the ratio

$$\xi = \frac{\ln \frac{\Gamma_{E_1}(x_1)}{\Gamma_{E_1}(x_2)}}{\ln \frac{\Gamma_{E_2}(x_1)}{\Gamma_{E_2}(x_2)}} = \frac{\sigma(E_1)}{\sigma(E_2)}$$

from the electron fluxes for two instants $t_1$ and $t_2$ sufficiently distant and corresponding to two spacecraft positions $x_1$ and $x_2$

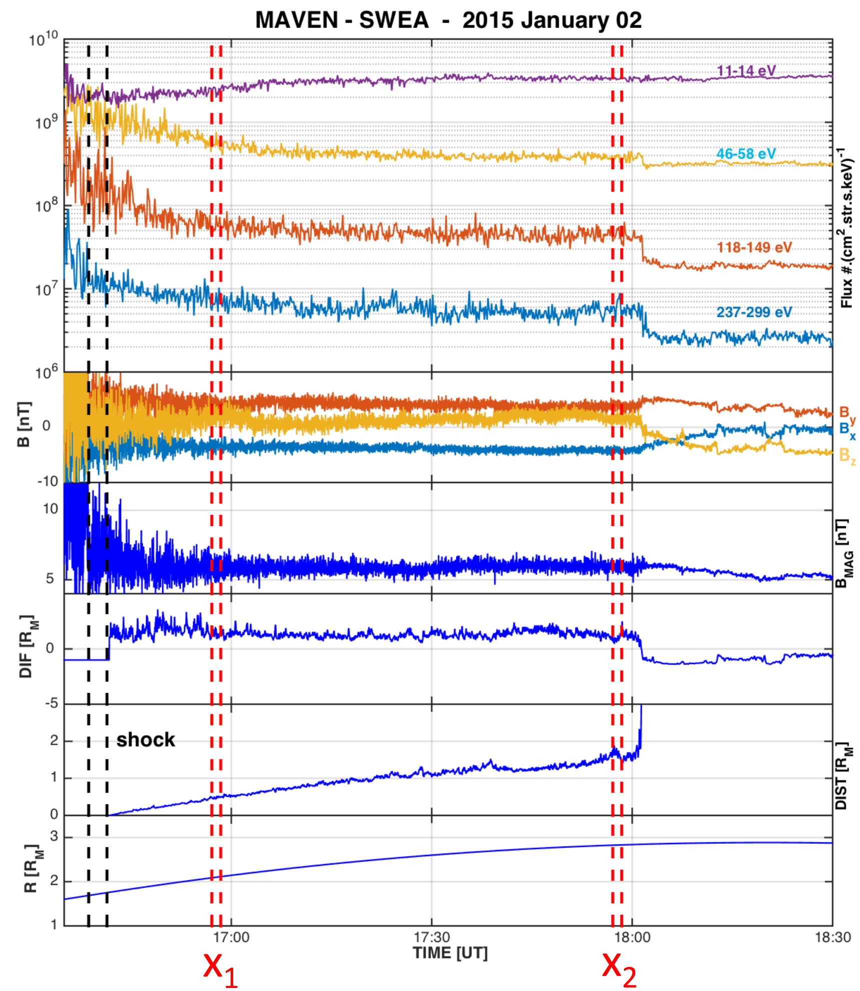

# Comparison with different profiles of EII cross-sections

The variation of $\xi_{E_0}(E)$ for $E_0$ = 52.1 eV (black closed circles) for two events are compared with the electron-Atomic hydrogen cross sections ratio $\left(\frac{\sigma(E)}{\sigma(E_0)}\right)$ from different available cross-sections in the literature.

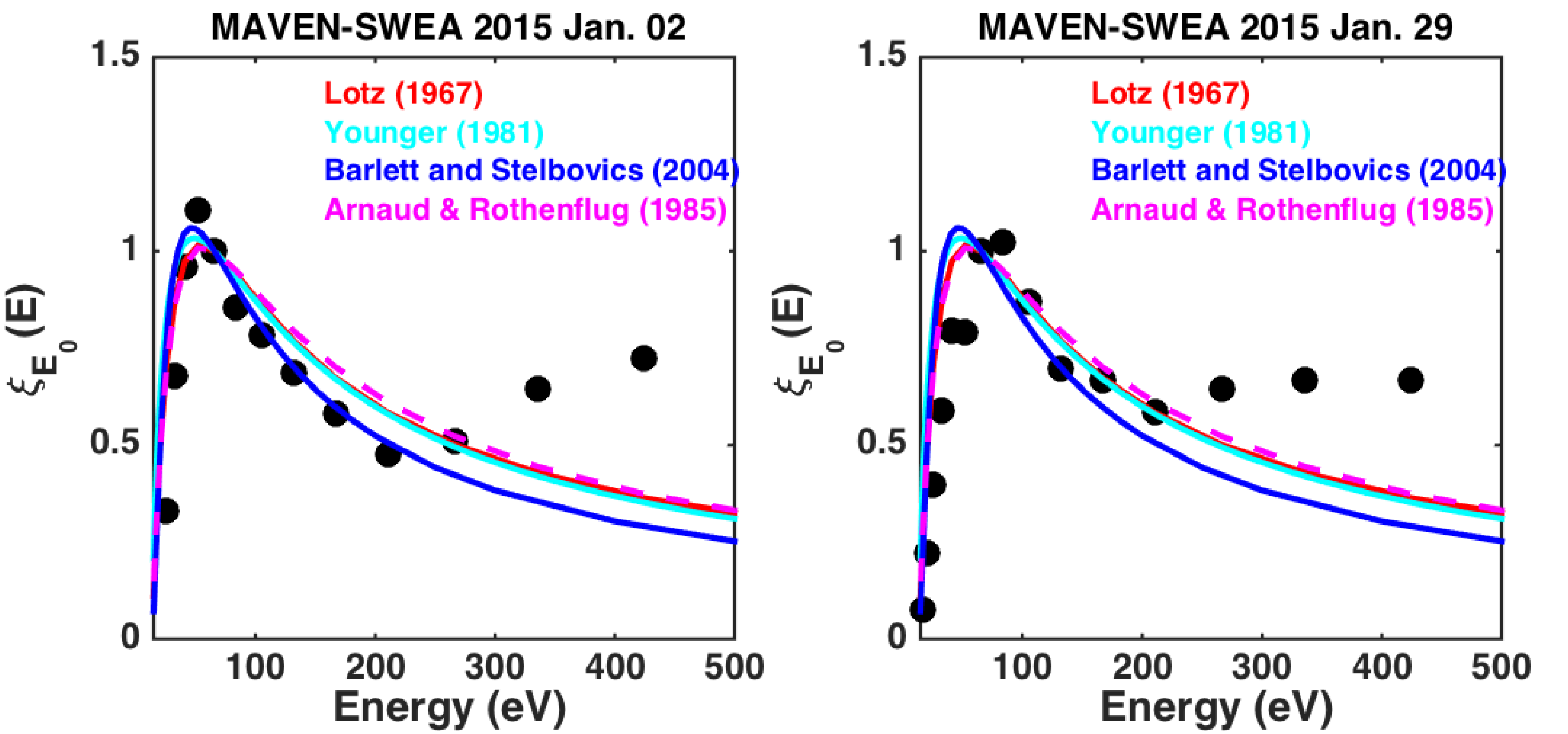


**As predicted by the present model, the empirical cross section tracks well the observed flux ratio for electron energy E ≤ 250 eV (lack of impact on oxygen? )**

Mazelle *et al.*, *Geophys. Res. Lett.*, 2018

# Conclusion: Martian Electron Foreshock

- Apparent discrepancy with the terrestrial 'paradigm' for the backtreaming electrons produced by Fast Fermi acceleration.
- Flux fall-off of the foreshock electrons is well reproduced by a simple 1-D analytical model describing the effect of **impact ionization on neutral exospheric hydrogen atoms.**
- This is the **first evidence** of this process upstream from the bow shock of Mars where it is usually neglected in the models.
- A complete calculation could be made using a more realistic 3-D model of the neutral hydrogen density.
- Conversely, the foreshock electron fluxes fall-off could be used **to put constraint on the local hydrogen density profile at high altitudes.** For every MAVEN orbit crossing the bow shock, a large part of the upstream path is inside the electron foreshock.
- It plays a role by increasing the production of **pickup protons** (and subsequent 'proton cyclotron waves') which are both related to atmospheric escape.

Mazelle *et al.*, *Geophys. Res. Lett.*, in press, 2018